

Detection of coherent acoustic oscillations in a quantum electromechanical resonator

Florian W. Beil

Center for NanoScience and Sektion Physik, Ludwigs-Maximilians-Universität, Geschwister-Scholl-Platz 1, 80539 München, Germany

Robert H. Blick^{a)}

Department of Electrical and Computer Engineering, University of Wisconsin-Madison, 1415 Engineering Drive, Madison, Wisconsin 53706

Achim Wixforth

Lehrstuhl für Experimentalphysik I, Universität Augsburg, Universitätsstraße 1, 86159 Augsburg, Germany

Werner Wegscheider and Dieter Schuh

Institut für Angewandte und Experimentelle Physik, Universität Regensburg, 93040 Regensburg, Germany

Max Bichler

Walter Schottky Institut, Am Coloumbwall 3, 85748 Garching, Germany

(Received 20 September 2006; accepted 18 December 2006; published online 22 January 2007)

Coherent control of occupation numbers in quantum mechanical multilevel systems is widely studied driven by its application in lasers and its prospects for quantum computational elements. Here the authors present a nanoelectromechanical resonator equivalent to the coherent control of a quantum mechanical two level system. The distinct eigenmodes of a nanomechanical beam resonator represent the two levels whose amplitude mode occupation numbers are controlled by a frequency matched acoustic excitation, mediated by a pulsed surface acoustic wave. They show that similar to quantum mechanical systems it is possible to transfer occupation numbers from one mode to another by matched acoustic pulses. © 2007 American Institute of Physics. [DOI: 10.1063/1.2432954]

A straightforward method to control occupation numbers in quantum mechanical two level systems is to apply short pulses of light, which are frequency matched to the transition frequency between the two levels.¹ The transfer of occupation number between two levels, usually termed as Rabi oscillations, relies on a system's state which can be described as a superposition of distinct modes, attributed eigenstates, being coupled by an external perturbation of the system. This pumping of atoms into an excited state results in an occupation inversion, which is the precondition for lasing operation.

Consequently, a mechanical analog can be realized once eigenstates are identified and appropriately addressed. For quantum electromechanical (QEM) systems, such as nanomechanical resonators, the different eigenstates correspond to different vibrational modes. Any displacement of the resonator can be described as a superposition of eigenmodes, whereas each eigenmode j contributes with an amplitude or, in analogy to the quantum mechanical counterpart, mode occupation number A_j to the overall motion. Usually, it is not possible to directly control the mode occupation numbers A_j , since thermal noise or nonlinear coupling determines the mode distribution. In the macroscopic extreme classical coupling of modes can occur for suspension bridges due to pulsed wind excitation, as the Takoma bridge disaster has shown² or due to pedestrians crossing the Millenium Bridge in London.³

In the experiment described here a surface acoustic wave (SAW) of Rayleigh type,⁴ properly described as a *nano-quake*, on GaAs is frequency matched to the transition fre-

quency between two eigenmodes of a nanomechanical beam resonator (see Fig. 1).⁵ In full equivalence to atoms pumped by light, the resonator represents the multilevel system, whereas the phonons excited by the acoustic wave correspond to the photons. The amplitude of the resonator beam's first eigenmode shows similar behavior as observed for occupation numbers in the quantum mechanical equivalent, namely, Rabi-like oscillations versus pump power and a Rabi-like splitting.⁶

To demonstrate the mechanical equivalence to pumped atoms, the suspended, gold covered nanobeam is placed in the line of fire of the interdigitated transducer (IDT) generating the SAW. The comblike IDT structure allows generation of SAWs by the inverse piezoelectric effect, which converts an applied radio frequency (rf) signal to the electrodes into mechanical stress, as the electric potential drops between each finger pair. If the frequency f_{SAW} of the signal meets the resonance condition $f_{\text{SAW}} = v_{\text{SAW}}/\lambda$, a coherent acoustic sound wave is generated. The IDT, however, provides a certain bandwidth, being determined by the number of finger pairs, hence allowing for a moderate frequency tuning, as employed in Fig. 3, for example, Ref. 5. The frequency is defined by the sound velocity $v_{\text{SAW}} = 2865 \text{ m s}^{-1}$ and the lithographically defined SAW wavelength λ (corresponding to the pitch between the SAW electrodes). As the length of the beam L is matched to $\lambda/2$, the two clamping points move in counterphase and the beam is periodically stressed by this motion.

The setup is placed in a strong magnetic field, which allows magnetomotive excitation and detection of the beam's off-plane eigenmode.⁷ Driving an alternating current at frequency f with power P_{res} along the conduction top metallic

^{a)} Author to whom correspondence should be addressed; electronic mail: blick@engr.wisc.edu

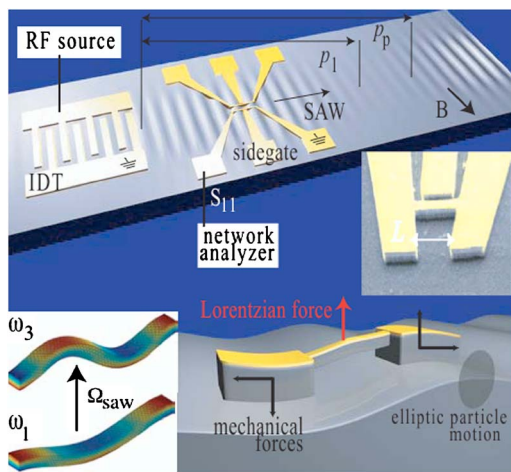


FIG. 1. (Color online) Top and lower right show setup of the experiment. The suspended beam is placed in the line of fire of a transducer which generates a surface acoustic wave (SAW) of frequency f_{saw} . The SAW displaces the anchoring points of the resonator beam in counterphase and periodically stresses the beam. The inset right of the center shows an actual SEM micrograph of the resonator beam and the clamping points. An in-plane magnetic field B allows detection of the beam's off-plane eigenmode by impedance spectroscopy. Lower left: schematic representation of the SAW induced pumping from the first to the third eigenmode of the beam $\omega_3 - \omega_1 = \Omega_{\text{saw}}$.

layer causes a Lorentz force, which when in resonance excites the beam's mechanical modes with an amplitude A . In Fig. 2(a) we traced the power dependence of this amplitude with $A = A_{\text{res}}$. The induced motion changes the beam's acoustoelectrical impedance Z_{beam} , which we measure as an effective amplitude of the oscillations $A = A_{\text{osc}}$ in Fig. 2(b). In turn it exhibits a mechanical resonance in the reflected power. Measuring the scattering parameter $S_{11} \sim (1 - A_{\text{osc}})$ versus driving frequency f reveals the fundamental mechanical resonance, shown in Fig. 2.

For large amplitudes $A \sim A_{\text{res}}$, nonlinear effects come into play and distribute energy among the beam's eigenmodes. This is shown in Fig. 2(a), where we plot A_{res} against the probe power P_{res} applied at the beam. Above $P = -56$ dBm nonlinear effects kick in and higher eigenmodes are excited ($A_{\text{res}} \sim A_1 + A_3$). The necessary adjustment of the SAW frequency $\Omega_{\text{saw}} = 2\pi f_{\text{saw}}$ to the transition frequency of the beam's first eigenmode to its third harmonic $f_{\text{trans}} = f_3 - f_1 \sim \omega_3 - \omega_1 = \Omega_{\text{saw}}$ was calculated by finite element simulations, achieving sufficient accuracy for the IDT's bandwidth (Fig. 1).

For pumping the transition from the first to the third eigenmode, short acoustic pulses were applied. The minimal pulse length is determined by the pitch of the IDT and is of the order of 100 ns. In Fig. 2(b) $A = A_{\text{osc}} \sim A_1$ exhibits oscillations against increased SAW pulse amplitude A_{saw} . This effect is best visualized when coding the reflected signal from the beam in a grayscale plot [Fig. 2(c)]. These oscillations of $S_{11} \sim (1 - A_{\text{osc}})$ vs A_{saw} are equivalent to oscillations of occupation numbers in a two level system usually plotted versus pump power; hence we term these oscillations as *acoustical Rabi-like oscillations* (AROs). Increasing the magnetoimpedance probe power P_{res} , the AROs disappear when increasing the power above the limit of nonlinear response at -56 dBm [Fig. 2(b)]. P_{res} corresponds to the power of the network analyzer applied to the sample.

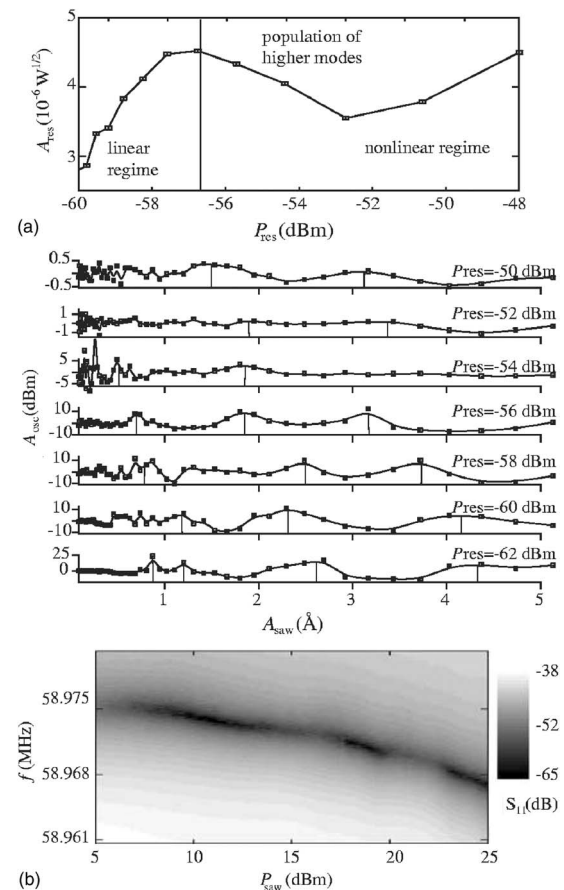


FIG. 2. (a) Dependence of the resonator oscillation amplitude $A = A_{\text{res}}$ on the applied magneto impedance probe power P_{res} . Above -56 dBm the nonlinear coupling to higher modes leads to a deviation from the linear increase. (b) Upper part: amplitudes $A = A_{\text{osc}}$ of acoustic Rabi-like oscillations (ARO) for different probe powers P_{res} . The AROs start to vanish for probe powers above the nonlinear limit of -56 dBm. Lower part: visualization of the ARO in the reflectance $S_{11} \sim (1 - A_{\text{osc}})$ at the beam vs acoustic pulse power P_{saw} . In this plot an increased modal occupation $A \sim A_1$ corresponds to darker areas, whereas the lighter regions correspond to low A_1 , due to acoustic coupling to a higher eigenmode A_3 .

Another characteristic feature which the quantum electromechanical resonator reveals is the characteristic dependence of the ARO on pump frequency f_{saw} as expected from quantum mechanical systems. In Fig. 3(a) the measured amplitude $A \sim A_1$ is plotted against a broad range of SAW frequencies. This shows that the observed mode coupling only occurs for a specific pulse center frequency $F_{\text{saw}} = f_{\text{trans}}$. Comparing the measured curve to the Fourier transform of the applied SAW signal A_{FT} at f_{trans} allows us to extract the transition frequency of the first to the third eigenmode to be 302.9 MHz, which lies in the active frequency range of the IDT. Here, we are able to cover a broader frequency range, since we operate the IDTs in pulsed mode. Hence, we find evenly spaced harmonics in the range of 280–340 MHz. The shape of A vs f_{saw} around the transition frequency for two different SAW powers shows the form of two separated resonances [Fig. 3(b)]. This again is expected for the coupling of two states leading to Rabi-like splitting of the energy levels.

To model acoustic pumping of mode transitions we adopt the theory developed for quantum mechanical systems to the acoustic case. The amplitude of the beam resonator's mechanical amplitude A in the linear regime is described as a superposition of eigenmodes A_j , whereas each mode j contributes to it with specific wave function shapes ψ_1 and ψ_3 .

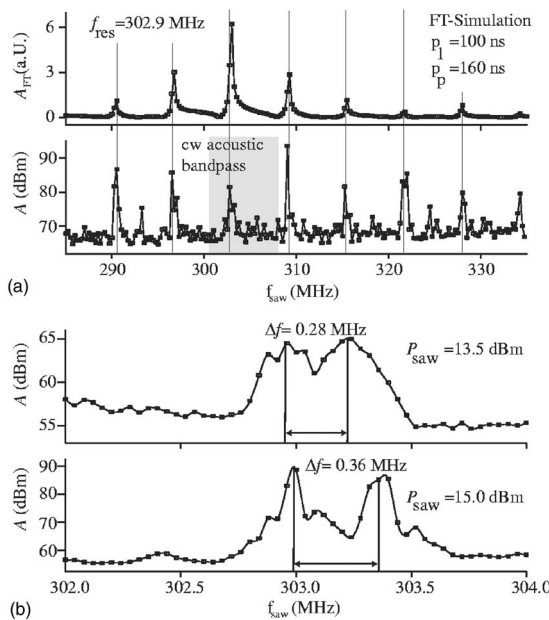


FIG. 3. (a) ARO vs SAW frequency f_{saw} and calculated component of the applied acoustic signal's Fourier transform (A_{FT}) at $f = f_{\text{trans}}$. From this f_{trans} is evaluated to $f_{\text{trans}} = 303.2$ MHz. (b) Measured amplitude A for f_{saw} close to f_{trans} for two different SAW pulse powers. The acoustic frequency splitting decreases for lower P_{saw} .

The SAW induced periodic stress acting on the beam is included in the Euler-Bernoulli beam equations by an additional term,^{8,9} which will make the A_j become time dependent. Using the orthogonality of eigenmodes¹⁰ in the rotating wave approximation,⁵ which assumes that contributions from eigenmodes with frequencies very different from $f_1 + f_{\text{trans}}$ can be neglected, we obtain the following coupled differential equation for the acoustically coupled eigenmodes A_1 and A_3 :

$$\frac{\partial^2 A_1}{\partial t^2} + 2i\omega_1 \frac{\partial A_1}{\partial t} = -\Omega_{13}^2 A_3,$$

$$\frac{\partial^2 A_3}{\partial t^2} + 2i\omega_3 \frac{\partial A_3}{\partial t} = -\Omega_{13}^2 A_1.$$

Here, $\omega_j = 2\pi f_j$, and Ω_{13} is the acoustic Rabi-like frequency, which is determined by the mass per unit length μ of the beam, the mismatch between the SAW frequency and the transition frequency $\Delta = f_{\text{trans}} - f_{\text{saw}}$.

$$\Omega_{13} = \int_0^L \psi_1 \frac{\partial^2}{\partial x^2} \psi_3 dx \frac{F_{\text{saw}}}{\mu} e^{i\Delta t}.$$

This integral depends on the mode shapes ψ_1 and ψ_3 of the two coupled modes integrated over the length L of the beam and the force F_{saw} the SAW exerts on the beam. The force can be calculated from simple beam theory with the assumption of elliptic motion of the suspension points with amplitude A_{saw} .

The two coupled modes will periodically exchange energy, whereas the acoustic Rabi frequency determines the period of this exchange. The amplitude of the SAW can be estimated by the acoustic power injected by the IDT, leading to typical frequencies of Ω_{13} in the megahertz regime. This corresponds to the observed Rabi-like splitting in Fig. 3, which allows direct evaluation of Ω_{13} . Solving the coupled differential equation [Eq. (1)] leads to the theoretical curves

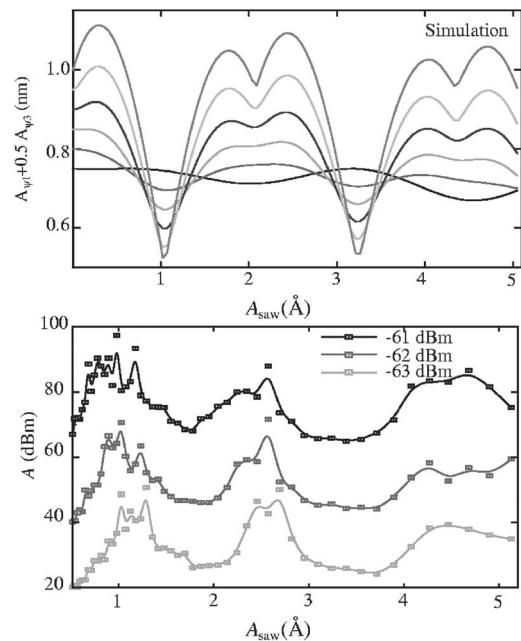


FIG. 4. Simulated (top) and measured (bottom) AROs in amplitude A . To model a contribution from the third eigenmode to the reflected signal to the first one, a superposition of $A \sim A_1 + 0.5A_3$ was calculated for different SAW pulse amplitudes. The simulation shows vanishing ARO for increased occupation of A_3 compared to A_1 , as observed in Fig. 2(a).

shown in Fig. 4. For the different traces the parameters A_1 and A_3 are varied in combination as $A_1 + 0.5A_3$, ensuring that the fundamental mode at A_1 and the higher harmonic at A_3 are excited. The calculations resemble the experimentally observed ARO in Fig. 4 for the range of applied SAW amplitudes.

In summary, we demonstrated that in analogy to the control of occupation numbers in a quantum mechanical two level system, the mode occupation numbers in quantum electromechanical resonators can be controlled by pulsed acoustic excitation. Hence, it is possible to coherently control the mode occupation numbers in a nanomechanical resonator, which can be exploited for achieving occupation inversion necessary for a mechanical equivalent to lasers, termed the “phaser.”

This work was supported by the Deutsche Forschungsgemeinschaft (BI-487/3) and the Air Force RSO (F49620-03-1-0420).

¹A. Zrenner, E. Beham, S. Stuffer, F. Findeis, M. Bichler, and G. Abstreiter, *Nature* (London) **418**, 612 (2002).

²K. Y. Billak and R. H. Scanlan, *Am. J. Phys.* **59**, 118 (1991).

³S. H. Strogatz, D. M. Abrams, A. McRobie, and B. Eckhardt, *Nature* (London) **483**, 43 (2005).

⁴L. D. Landau and E. M. Lifshitz, *Theory of Elasticity* (Butterworth-Heinemann, Oxford, 1999), Vol. 1, p. 97.

⁵A. Wixforth, J. Scriba, M. Wassermeier, J. P. Kotthaus, G. Weimann, and W. Schlapp, *Phys. Rev. B* **40**, 7874 (1989).

⁶I. I. Rabi, N. F. Ramsey, and J. Schwinger, *Rev. Mod. Phys.* **26**, 167 (1954).

⁷R. H. Blick, A. Erbe, L. Pescini, A. Kraus, D. V. Scheible, F. W. Beil, E. M. Höbberger, A. Hoerner, J. Kirschbaum, H. Lorenz, and J. P. Kotthaus, *J. Phys.: Condens. Matter* **14**, R905 (2002).

⁸K. Magnus and K. Popp, *Schwingungen* (Teubner, Stuttgart, 1997), Vol. 1, p. 15.

⁹K. F. Graff, *Wave Motion in Anelastic Solids* (Ohio State University Press, Columbus, 1975), Vol. 1, p. 42.

¹⁰C. Cohen-Tannoudji, *Quantum Mechanics* (Wiley, New York, 1996), Vol. 2, p. 137.